Anti-scaling and Water Flux Enhancing Effect of Alginate in Membrane Distillation

Elizabeth Arkhangelsky[1#], Filicia Wicaksana[2#*], Rong Wang[3,4*]

[1] Department of Civil and Environmental Engineering, Nazarbayev University, 53 Kabanbay Batyr Avenue, Nur - Sultan 010000, Kazakhstan

[2] Department of Chemical and Materials Engineering, the University of Auckland, Auckland 1142, New Zealand

[3] School of Civil and Environmental Engineering, Nanyang Technological University, 639798 Singapore, Singapore

[4] Singapore Membrane Technology Center, Nanyang Technological University, 639798 Singapore, Singapore

[#]These authors contributed equally to the manuscript

[*]Corresponding authors:

Engineering Block 5 – Building 405, 5 Grafton Road

Department of Chemical and Materials Engineering,

the University of Auckland

Auckland 1010, New Zealand

Tel: +64 9 923 1861

Email address: f.wicaksana@auckland.ac.nz (F. Wicaksana)

Email address: rwang@ntu.edu.sg (R. Wang)

Abstract

This study focused on the effect of sodium alginate on the performance of direct contact membrane distillation (DCMD). The feed solution contained various combinations of sodium chloride, sodium sulfate and calcium chloride along with bovine serum albumin, xanthan gum and sodium alginate. Unlike findings from the majority of prior studies that suggested the presence of alginate in feed solution caused the deterioration of membrane process performance, our results indicated that sodium alginate exhibited anti-scaling properties and water flux enhancing effect. However, this interesting phenomenon was exhibited by sodium alginate under particular conditions only. Experiments performed with other organic foulants such as xanthan gum did not display the same trend. It is believed that the presence of a hydrophilic layer (calcium alginate gel), which is much less thermal conductive as compared to the PTFE membrane, on the top of the membrane could reduce the amount of heat dissipated due to evaporative cooling or reduce conductive heat loss in the membrane, thus enhancing the thermal efficiency of the system.

***Keywords*:** membrane distillation; alginate; salts; anti-scaling; water flux enhancing effect.

1. Introduction

Membrane distillation (MD) process was introduced in the late 1960s [1, 2]. MD has a wide range of potential applications, such as sea/brackish water desalination, wastewater treatment and food processing. MD has an important advantage that enables coupling with waste heat or renewable energy sources, such as geothermal or solar energy. Other advantages include the ability to operate at relatively mild temperatures (50–80°C) and high salt concentrations, as well as the ability to operate intermittently without causing membrane damage [3, 4].

Although fouling in MD is less severe than in pressure-driven membrane processes, deterioration of the process performance due to fouling remains one of the main issues in MD process. The presence of algal organic matters (AOM) produced by marine phytoplankton in seawater desalination process is unfavorable as it could adversely affect the membrane performance [5]. Sodium alginate is commonly used to simulate biofouling due to AOM. Despite this critical issue, there are only limited studies on alginate fouling in MD process with various outcomes. The work by Naidu et al. showed that the presence of alginic acid in the feed solution led to 44.1% decrease in direct contact MD (DCMD) process performance; interestingly, when alginic acid was mixed with other organic foulants (bovine serum albumin (BSA) and humic acid), a stable permeate flux could be maintained for a longer time as compared to MD processes with individual foulants, although subsequently the permeate flux experienced sharp decline. It was stated that the interaction between foulants caused the individual organic compounds to behave differently when mixed together [6]. Liu et al. studied the fouling mechanism in MD by focusing on the effect of feed properties and charges [7]. Various compositions of BSA+sodium alginate (ALG) and lysozyme (LYS)+ALG feed solutions were tested. It was found that when present individually, BSA and ALG enhanced

the severity of fouling due to conformational changes during the feed heating process. They further indicated that when the feed contained both BSA and alginate, the presence of ALG resulted in the formation of dense gel-like layer that prevented more BSA to deposit on the membrane surface, thus delaying further decline in permeation flux of BSA/ALG mixed feed solution.

There have been a limited number of studies that suggest alginate could display a certain degree of antifouling properties [8-10]. Zhou et al. showed that polyelectrolyte multilayers containing chitosan and alginate on top of biocompatible poly(lactide-co-glycolide) nanoparticles had potential as antifouling coatings by preventing interaction with proteins [10]. In 2010, Higgin at al. discovered that a feed containing silica and alginate could mitigate RO membrane scaling [8]. In another work, the ionic composition, particularly Ca^{2+}, had been shown to play an important role in alginate-alginate interactions that governed the reversibility of alginate fouling layer on polyamide reverse osmosis (RO) membrane [11]. Mo et al. reported that the addition of calcium up to a certain concentration level in the feed solution containing 20 mg/l of alginate could slow down the fouling of nanofiltration (NF) membrane [9]. The authors further suggested that a sufficiently high calcium concentration in the aforementioned feed solution could facilitate the formation of aggregates, which reduced the gel layer formation and slowed down the initial flux decline due to the reduction of the effective convective mass transfer of alginate toward the membrane surface.

The above-mentioned prior works indicate the lack of detailed fouling studies in MD process, particularly on the interaction between ionic compounds in feed solution containing alginate. The work presented in this paper involves systematic studies on the impact of alginate on the behavior of thermally driven membrane process by using several combinations of foulants at

various ionic strengths (salinity levels). Rheological study and visual observation were also performed to support the findings. To the best of our knowledge this is the first study that reports anti-scaling and water flux enhancing effect of alginate in membrane processes.

2. Materials and Methods

2.1. Membrane, MD setup and experiments

Polytetrafluoroethylene (PTFE) membranes used in the study were supplied by GE Energy. The flat sheet membrane has 0.12 - 0.22 mm thickness, 200 nm pore size and 3.5 bars liquid entry pressure, with an effective filtration area of 10 x 13 cm^2. The feed solution contained various combinations of organic and inorganic foulants that are commonly present in seawater to represent biofouling (due to extracellular polymeric substances or algal organic matters) and scaling. Inorganic foulants were prepared by mixing sodium chloride (NaCl), sodium sulfate (Na_2SO_4) and calcium chloride ($CaCl_2$) to achieve various salinity and $CaSO_4$ saturation levels, while organic foulants were sodium alginate (ALG), BSA and xanthan gum (XG). Detailed compositions of feed solution used for fouling experiments are presented in Table 1. BSA, XG and $CaCl_2$ were purchased from Sigma-Aldrich, USA, while ALG and NaCl were purchased from Hayashi Pure Chemical Industries Ltd., Japan, and Merck, respectively.

Table 1. Composition of feed solutions used in the study (HS: high salinity; LS: low salinity).

Feed Solution	NaCl, g/L	$CaCl_2$, g/L	Na_2SO_4, g/L	$CaSO_4$ saturation, %	Organic foulant / concentration in ppm	Feed temperature, ˚C
HS 15%	35	1.81	2.32	15	0	70
HS 15% + ALG	35	1.81	2.32	15	ALG / 100	70
LS 15%	0.22	0.78	0.57	15	0	70
LS 15% + ALG	0.22	0.78	0.57	15	ALG / 100	70
LS 50%	0.61	2.13	1.56	50	0	70
LS 50% + ALG	0.61	2.13	1.56	50	ALG / 100	70
LS 100%	1.11	3.88	2.84	100	0	70
LS 100% + ALG	1.11	3.88	2.84	100	ALG / 100	70
ALG	0	0	0	0	ALG / 100	70
LS 100% + BSA	1.11	3.88	2.84	100	BSA / 100	70
LS 100% + XG	1.11	3.88	2.84	100	XG / 100	70
LS 100% + ALG	1.03	3.59	2.63	100	ALG / 100	55
LS 100% + ALG	0.95	3.3	2.42	100	ALG / 100	40

The equipment setup used for DCMD experiments is depicted in Figure 1. Two variable-speed *Masterflex* peristaltic pumps were used to circulate the feed and cool side streams counter-currently through the membrane holder at the same cross-flow velocities. Commercial diamond-patterned spacers were placed on both sides of the membrane. The inlet temperatures of feed (70, 55 or 40˚C) and cool side streams (20˚C) were kept constant throughout the MD process. The feed concentration was maintained constant by manually topping up the feed on regular basis. The working volume of the feed tank was 6.5 L. An electronic balance (*Mettler Toledo,* Switzerland) connected to a data logging system was used to record the water flux (*J*)

at predetermined time intervals. Each experiment was carried out in DCMD configuration for 7 hours with a new membrane. A series of MD runs were performed with MilliQ water as feed to evaluate the MD flux behavior without the presence of salt/foulants. Unless otherwise specified, the experiments were conducted with spacers on both sides of the membrane under the following conditions: cross-flow velocity of 15 cm/s; feed side temperature of 70˚C; permeate side temperature of 20˚C. The experiments were replicated to ensure the reproducibility of results.

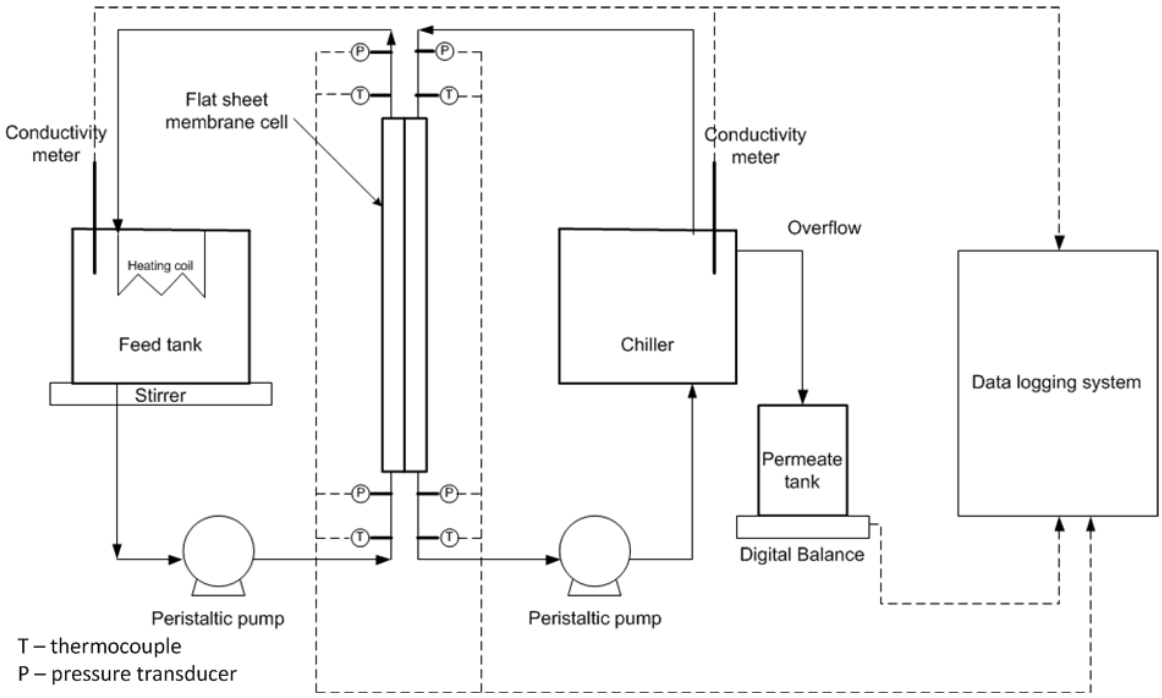

Figure 1. Schematic diagram of bench scale membrane distillation system.

2.2. Visual observation, viscosity and contact angle analysis

Keyence VHX 500F digital microscope and a digital camera (*Samsung*) were used to capture the images of pristine and fouled membrane surfaces for visual observation. The

measurements of hydrophobicity/hydrophilicity of both pristine and fouled membranes were carried out by using *optical contact angle 20* from *Dataphysics*, Germany. The rheological behavior was studied by using *Physica MCR 101* rheometer (*Anton Paar GmbH*, Austria) equipped with a stainless steel cone of 49.973 mm diameter and 0.985º angle.

3. Results and Discussion

Results obtained from MD experiments are shown in Figures 2-13. It is important to note that no membrane wetting was observed during all MD experiments performed in this study. The permeate conductivity remained constant throughout all experimental runs (~ 2 µS/cm), which confirmed that no wetting occurred.

3.1. Flux enhancement by alginate and the effect of ionic strength

The permeate flux profiles at different feed salinity levels (ionic strengths) on MD performance can be seen in Figure 2. Both high and low salinity feed solutions did not exhibit any water flux decline throughout 420 minutes of operation, while the addition of 100 ppm sodium alginate into the feed resulted in 25% flux decline for high salinity feed (the flux dropped from 20 LMH to 15 LMH) and 15% for low salinity feed (the flux dropped from 33 to 28 LMH). This is expected since alginate is known as fouling precursor in various membrane processes including membrane distillation [6, 12-14]. However, it is interesting to observe that the presence of sodium alginate in low salinity feed has magnified the initial water flux by 1.4 times (Figure 2b) (24 vs. 33 LMH). Further experiments were then performed to investigate this interesting phenomenon.

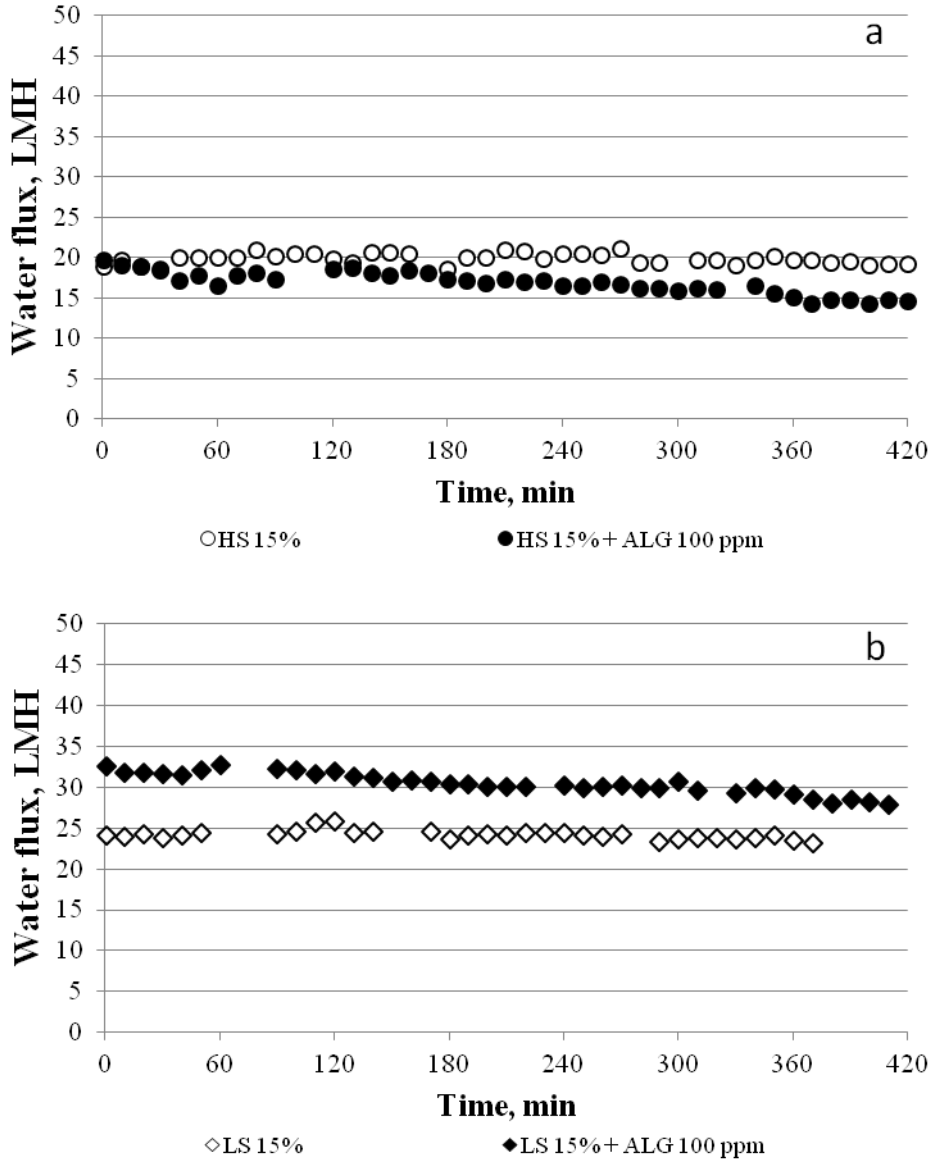

Figure 2. Permeate flux profiles at different ionic strengths (a. high salinity feed (HS); b. low salinity feed (LS); feed side at 70°C and cool side at 20°C).

Figure 2 also indicates that higher feed ionic strength resulted in lower permeate flux. The increase in ionic strength from 0.037 M (LS 15%) to 0.696 M (HS 15%) reduced the permeate

flux from 24 LMH to 20 LMH (16.7%). A similar trend can also be seen in Figure 3. This can be explained by the expression below [15, 16]:

$$p_w = P_w^*(1 - x_i)$$

where p_w is the partial vapor pressure of water, P_w^* is the vapor pressure of pure water, x_i is the mole fraction of solute in the solution.

According to Raoult's law, the presence of salt in the feed solution decreases the partial vapor pressure of water. Hence, lower permeate flux occurs due to the decrease in driving force. Our baseline test (MD process with MQ water as feed) also reflected this phenomenon. Due to relatively low ionic strengths of LS 15% and LS 50% ($\leq$ 0.1 M), their initial flux values (~ 24 LMH) were only slightly lower than the one with pure water as feed (24.5 LMH, as shown in Figure 8). More substantial drop in initial flux occurred when the ionic strength reached 0.18 M (LS 100%). Another contributing factor could be the changes in viscosity of the salt solutions. The presence of salts in the feed solution increased the viscosity from 1.7 Pa.s up to 11 Pa.s for HS15% (more detailed discussion on the effect of viscosity is given in section 3.7).

3.2. The effect of calcium sulfate saturation level

Figure 3 depicts the MD process performance for feed solutions with and without alginate at 50% and 100% $CaSO_4$ saturation levels. In contrast to 15% (Figure 2b) and 50% (Figure 3a) saturation levels, which showing no water flux decline, feed with 100% saturation led to 80% flux drop in the absence of alginate, suggesting fouling/scaling had occurred. With the presence of alginate, the initial water flux increased by 1.44 times for 50% saturation level

and 1.76 times for 100% saturation level. Unfortunately, the benefit of the initial flux increase was offset by the increase in fouling propensity as the percentages of flux decline were 15% for 50% saturation and 37% for 100% saturation. In fact, the increase in fouling propensity from 15% to 37% (~ 2.4x) was twice as much as the gain obtained from the initial flux increase (~ 1.2x). Nevertheless, the flux values throughout the MD process with the presence of alginate were still higher than those without alginate.

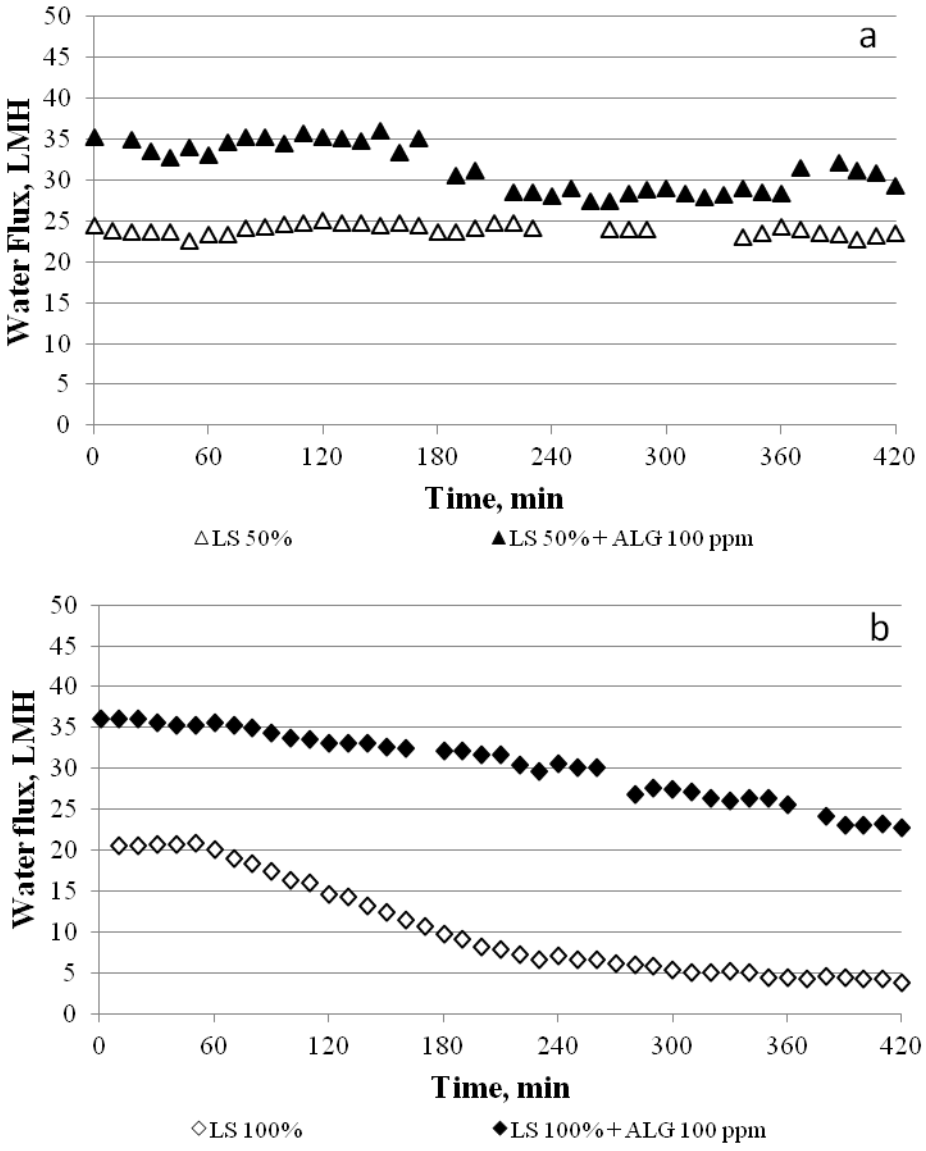

Figure 3. The influence of feed solution saturation level on MD process performance (feed side at 70^{o}C and cool side at 20^{o}C).

3.3. The effect of feed temperature

The effect of feed temperature on water flux is shown in Figure 4. Since membrane distillation is thermally-driven process, in which the increase in temperature difference between the feed side and the cool side will increase the vapor pressure difference (driving force), it is expected that higher permeate flux can be achieved at higher feed temperature (the permeate flux increased from 7 LMH at 40^{o}C to 13 LMH and 20 LMH at 55^{o}C and 70^{o}C, respectively). However, another interesting phenomenon was observed, with the increase in feed temperature from 40^{o} to 55^{o}C (Figure 4b) and 70^{o}C (Figure 3b), the flux values with the presence of alginate were higher than that of without alginate. Although the presence of alginate at 40°C did not alter the initial water flux value, it can be observed that the feed containing alginate could maintain the permeate flux at a relatively constant level throughout the seven hours of MD process. In the absence of alginate, the MD experienced 40% flux decline (Figure 4a). The MD run at higher temperatures also exhibited better performance with the presence of alginate. This suggests that alginate displays a certain degree of anti-scaling property that can be beneficial to membrane processes, particularly membrane distillation. Hence, the following studies were performed to obtain better understanding of this distinctive characteristic.

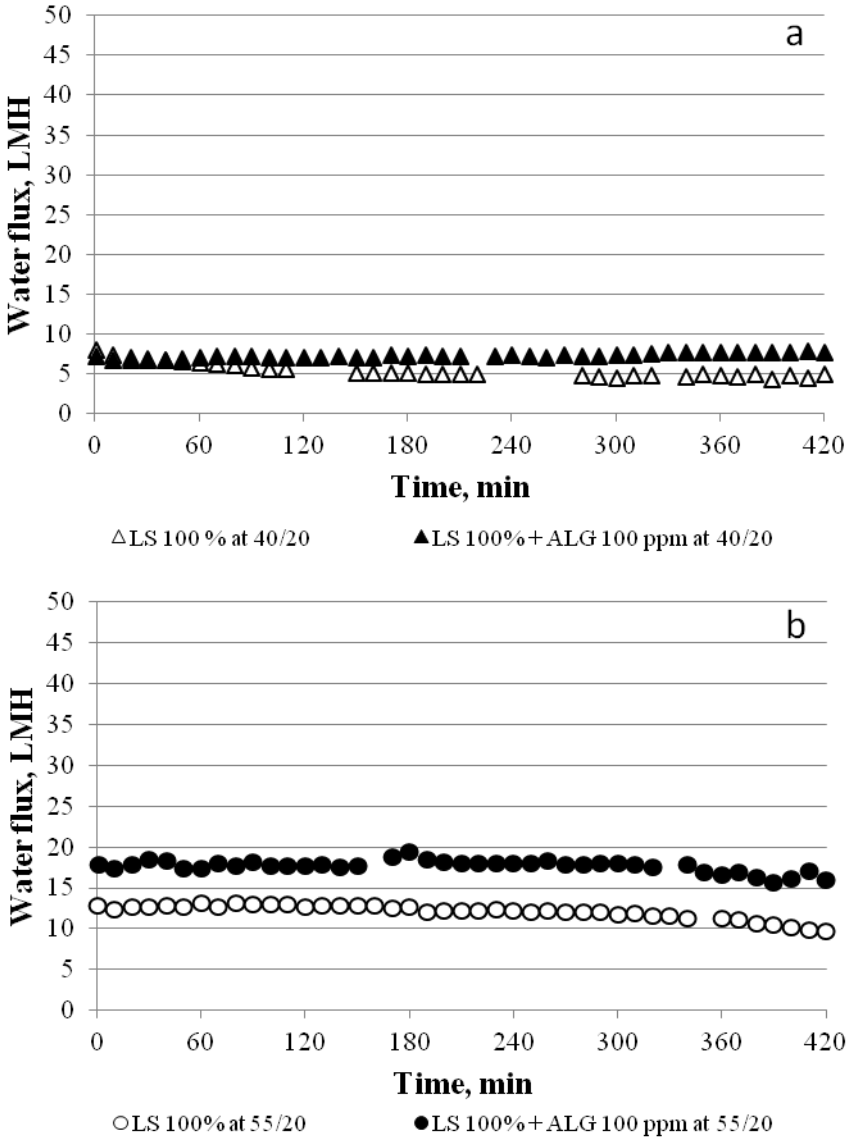

Figure 4. Effect of feed temperature on MD process performance.

3.4. The effect of alginate concentration

The influence of sodium alginate concentration on the MD process performance is summarized in Figure 5. It can be seen that the greatest flux enhancement effect of alginate was achieved with the addition of 100 ppm alginate (the initial flux increased from 20 LMH

without ALG to 36 LMH with 100 ppm ALG). It is also noticeable that the more alginate added into the feed solution (up to 60 ppm of alginate), the less severe the fouling. However, when the alginate added reached 100 ppm, the fouling severity started to increase, indicating that 60 ppm was a critical alginate concentration in this study. The changes in feed temperature will alter the feed viscosity, the solubility of salt, and the mass transfer in MD, that in turn will affect the kinetics and the amount of calcium alginate gel layer formed. Hence, it is expected that the critical alginate concentration will vary with the changes in feed temperature. Further study is required to determine how the critical alginate concentration will change with the changes in feed temperature.

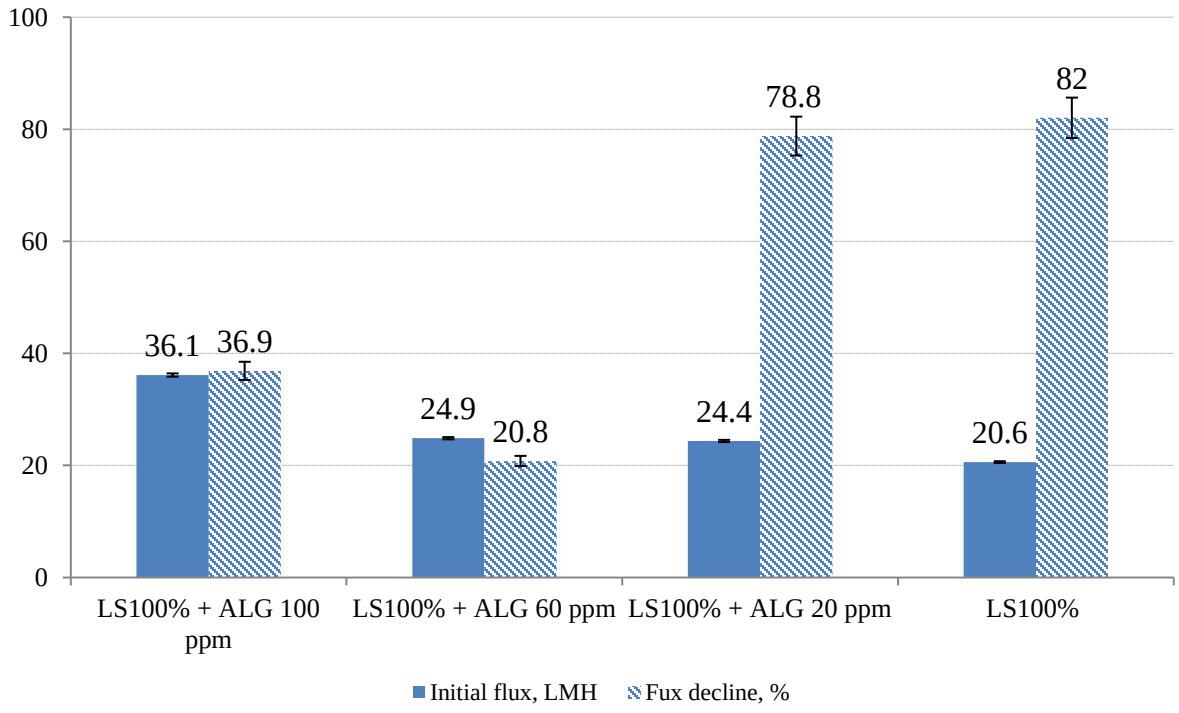

Figure 5. Impact of alginate concentration on MD process performance (feed side at 70°C and cool side at 20°C).

3.5. The effect of foulant types and membrane spacer

The effect of foulant characteristics on MD performance was studied by using xanthan gum (XG) and protein (BSA). Our results indicated that the presence of XG (Figure 6) did not alter the MD performance since the initial water flux and % flux decline were close to the one with salts only (initial water flux of ~20 LMH and 80% flux decline). Although ALG, BSA and XG were studied at the same concentration (100 ppm), there were other factors that determined the severity of fouling, such as the nature of foulant, temperature and interaction with other parameters. Severe fouling could occur with the presence of certain foulant at low concentration, while other type of foulant might require higher concentration to cause severe fouling.

Results in Figure 6 show that BSA has the lowest percentage (%) flux decline (7.2%) as compared to XG and alginate. BSA is widely known as fouling precursor. However, the severity of fouling caused by BSA could be affected by the presence of calcium and temperature. BSA can bind with ions such as Ca^{2+} present in the feed solution [17]. The binding reduced the amount of free calcium ions in the solution, thus suppressing the risk of scaling on the membrane surface. On the contrary, it was reported that conformational changes of BSA molecules could occur under thermal condition that could promote the aggregation of BSA in a solution containing calcium, thus increasing the fouling severity [7]. Nevertheless, the authors reported that the aggregation process was slow as more observable flux decline only occurred at a later stage of the MD process (after 1 day). Hence, the severity of fouling caused by BSA depends on which of the above-mentioned factors is more dominant. In addition to this, our experiment was only performed for 7 hours. Study on this

effect for long term experiment is required in future work to obtain better understanding of the governing factor.

Figure 6 confirms that among the three foulants tested in this study, only alginate displayed a water flux enhancing effect. The initial water flux values with BSA and XG were close to the one without the presence of these foulants.

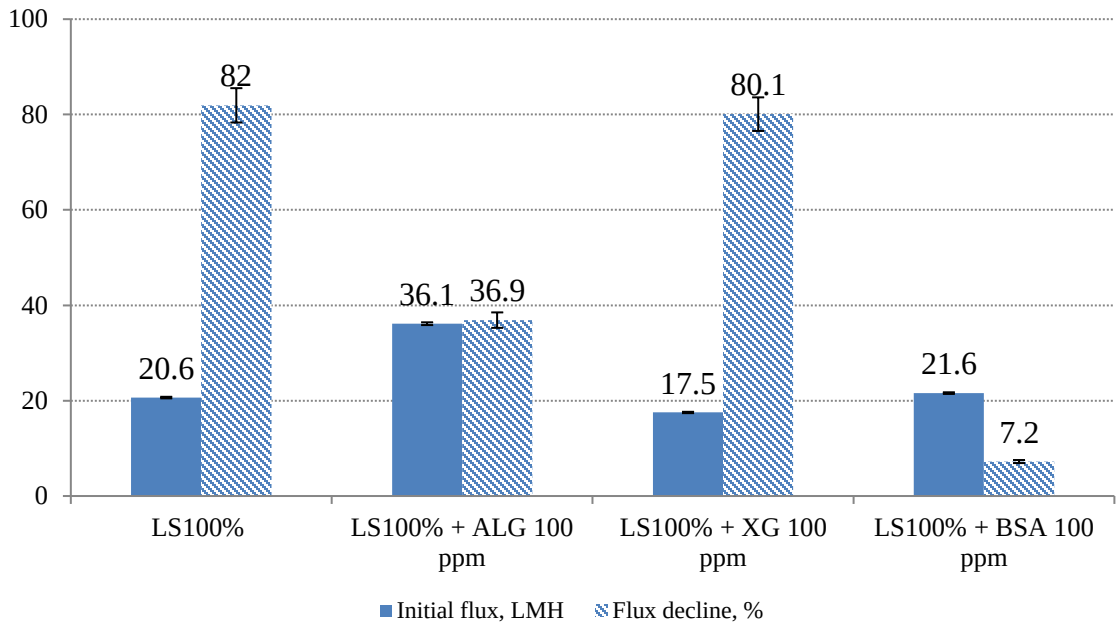

Figure 6. Influence of foulant nature on MD process performance (feed side at 70°C and cool side at 20°C).

It was found that the MD performance was also affected by the use of spacer (Figure 7). The feed was LS 100% + ALG 100 ppm. The absence of spacer on the feed side caused the initial flux to be lower than the one with spacer (25.8 LMH as compared to 36.1 LMH). The presence of spacer on the feed side helped to generate greater turbulence that disrupted the concentration polarization and/or temperature polarization, allowing greater increase in the initial flux. However, the increase in flux due to improved mass transfer led to greater amount

of foulants brought to the membrane surface, that eventually resulted in greater % flux decline for experiment with spacer as compared to the one without spacer (37% vs 21%).

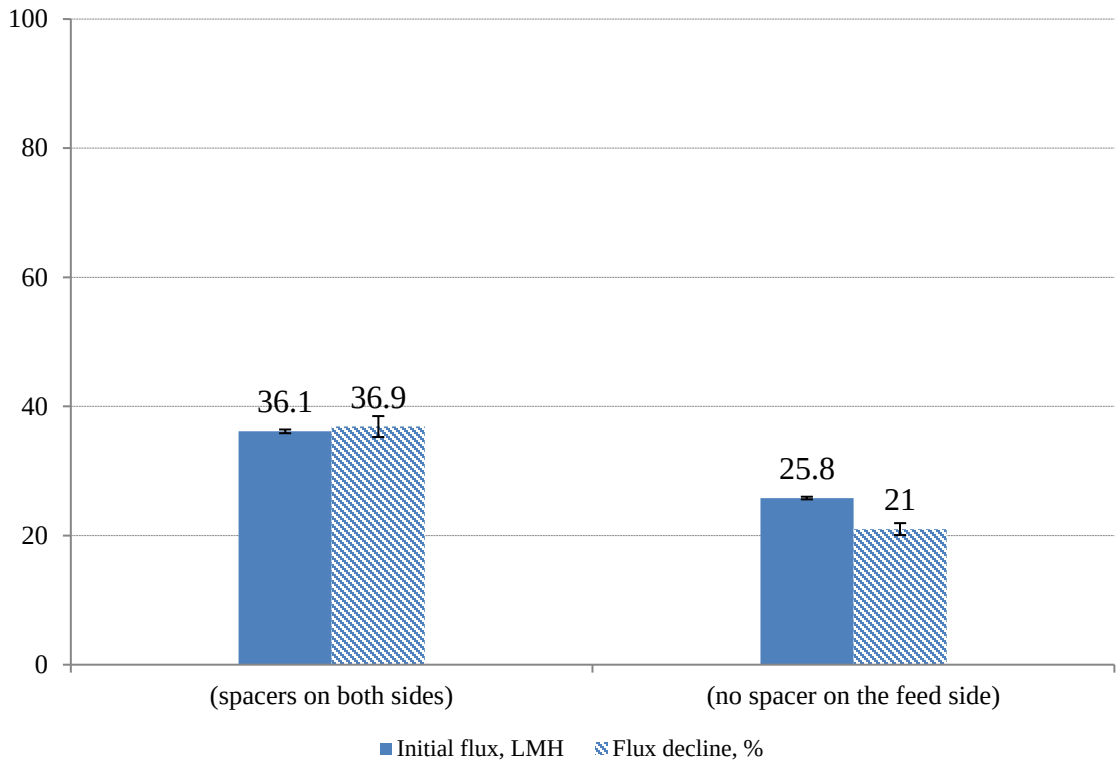

Figure 7. Comparison of MD performances with and without spacer for LS 100% + ALG 100 ppm (feed side at 70^{o}C and cool side at 20^{o}C).

3.6. Alginate injection time

Figure 8 compares the flux profiles of MD process with alginate already presence in the feed solution since the beginning of the process, to the one with alginate added later in the process (after 3 hours of operation). Although there was no sudden jump in the permeate flux upon alginate addition at 3 hours of MD operation, it appeared that the flux could be maintained at

~ 8 LMH after 420 minutes of operation as compared to ~ 4 LMH for the process without alginate (Figure 3b).

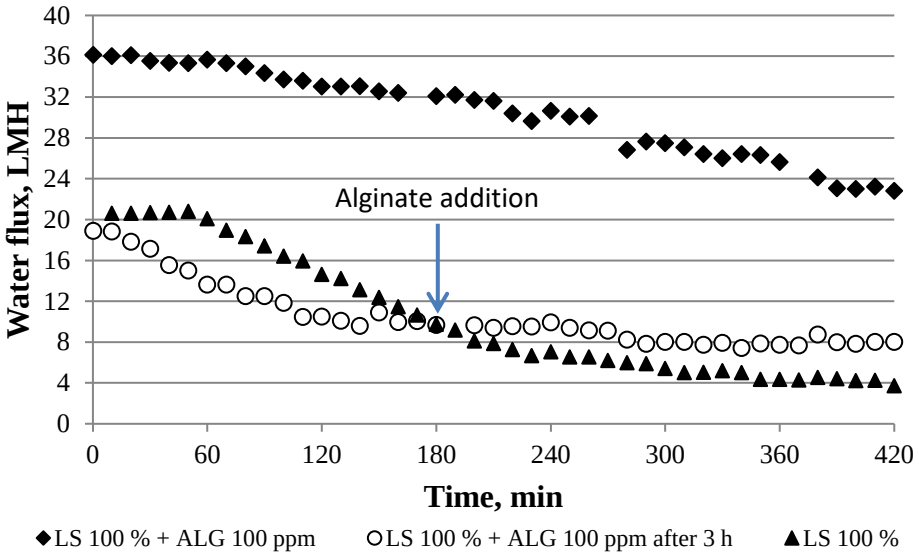

Figure 8. The effect of alginate injection time on MD process performance (feed side at 70°C and cool side at 20°C).

3.7. The effect of viscosity

Figure 9 compares water flux profiles of ultrapure water (MQ) and 100 ppm of alginate solution without salt. The water flux of alginate solution was lower than the one of pure water. This could be due to higher viscosity of alginate solution that influenced the boundary layer thickness and the heat transfer [18]. This result further suggests that the increase in the initial flux phenomenon only occurred when both calcium and alginate present in the feed solution since there was no initial flux increase when there was no calcium present in the feed solution.

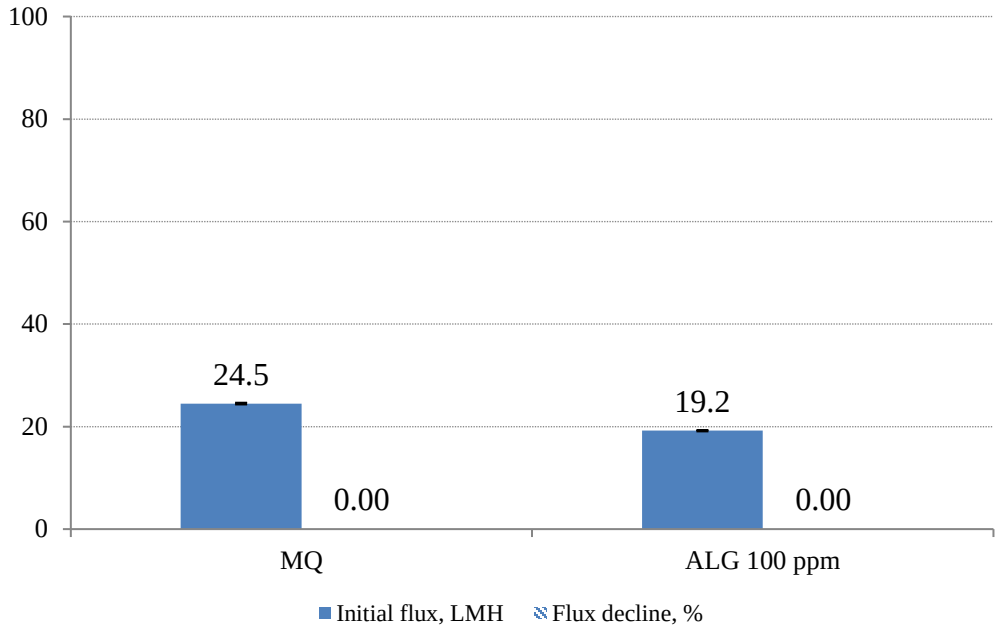

Figure 9. Comparison of MD performances with MilliQ water (MQ) and 100 ppm alginate solution as feed (ALG) (feed side at 70^{o}C and cool side at 20^{o}C).

Rheological behavior of feed solutions was studied within 0.001 – 1000 s^{-1} shear rate range at 70^{o}C (Figure 10). This temperature was selected to mimic the temperature of MD process. All solutions containing alginate exhibited reduction of viscosity with the increase in shear rate, while the viscosity of water remained constant at 0.001 Pa s. Unfortunately, the measured values could not represent the actual viscosity values of the mixtures. This was due to the formation of gel-like substance (calcium alginate). Hence, only the viscosity of the liquid phase that could be measured. Despite this issue, it can be seen that solutions with higher ionic strength display higher viscosity values that relate to the lower initial flux of HS 15% as compared to LS 15% (Figure 2). Similar viscosity values of LS 15%+ALG, LS 100%+ALG and ALG solutions indicated that the salt contents were relatively low to alter the viscosity

values (noting the above-mentioned issue that only the viscosity of liquid phase could be measured).

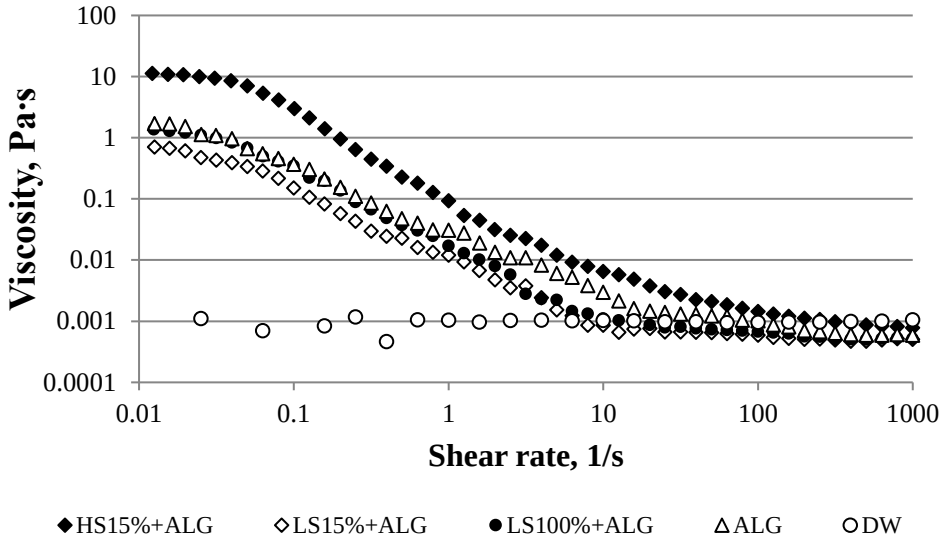

Figure 10. Viscosity of feed solutions as a function of shear rate.

3.8. Visual observation

Visual observations were performed by using a digital camera and a digital microscope to capture the images of pristine and used membranes upon experiments under various conditions (Figure 11). Despite no observable flux decline with both low and high salinity feed solutions at 15% saturation level (Figure 2a), a few salt crystals were found on the membrane surface with high salinity feed indicating the onset of fouling/scaling (Figure 11b), while there was no crystal present on the membrane surface with low salinity feed (Figure 11c). This was expected since the sodium chloride content in high salinity feed (35 g/L) was significantly higher than in low salinity feed (0.22 g/L), which was further concentrated

during MD process. The addition of alginate in low salinity feed solution caused the membrane to be covered by a gel-like substance upon MD process (Figure 11d). More gel aggregates were formed with higher feed ionic strength (Figure 12). Interestingly, there was not salt crystal formed on the membrane surface. It is widely known that calcium ions are able to form a cross-link with alginate molecules to produce water-insoluble gel-like aggregates [19]; thus higher calcium content in higher salinity feed solution enhanced the formation of gel aggregates. It was apparent that the formation of gel layer did not attribute to membrane fouling since the initial flux values were greater and the percentage (%) flux decline values were less than those without the presence of gel aggregates (Figures 2 and 3). One possible reason was that the binding caused the reduction of calcium ions and ALG present in the solution, thus minimizing the accumulation of less viscous ALG layer and calcium sulfate crystals on the membrane surface.

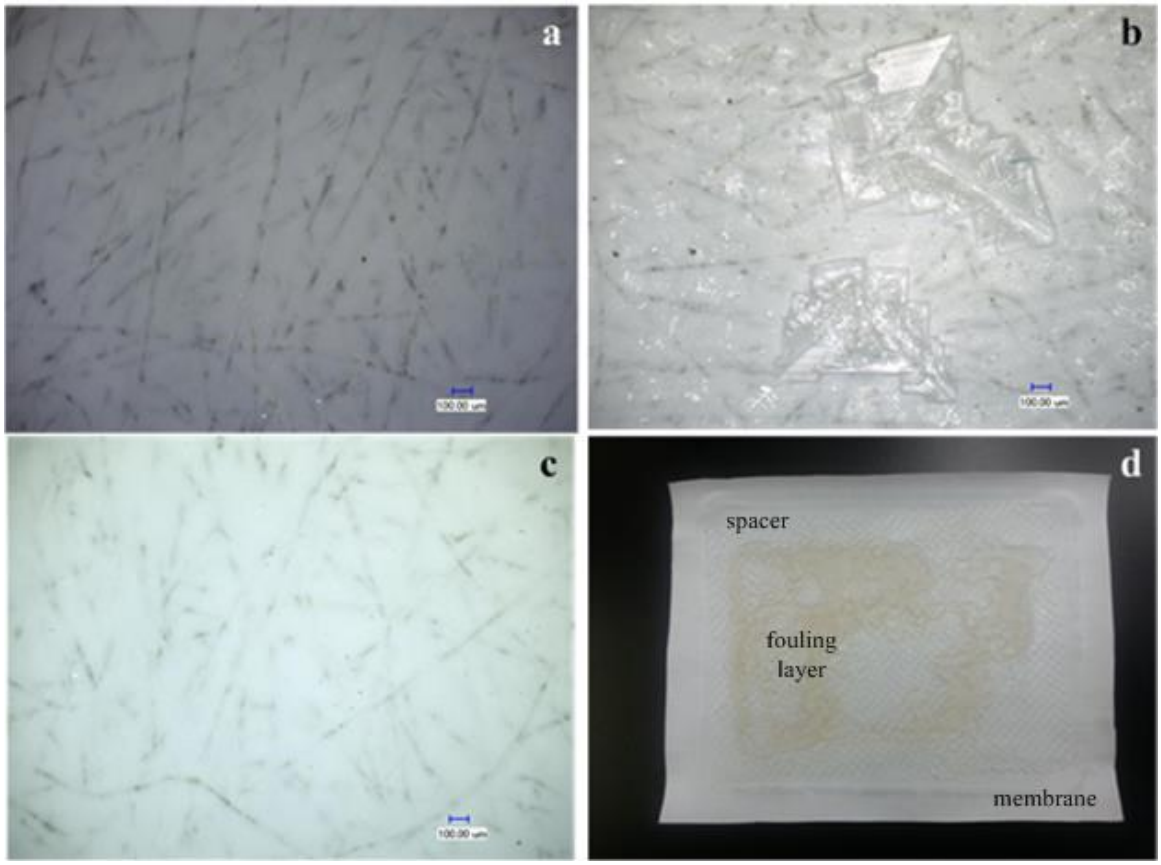

Figure 11. Digital images of membrane surfaces (a) pristine membrane; (b) upon experiment with HS 15%; (c) upon experiment with LS 15%; (d) image of the membrane with spacer upon experiment with LS 15%+ALG.

Figure 12 also shows that higher calcium content in feed led to a greater amount of gel aggregates formed. The gel became less watery when the temperature decreased from 70 to 40 ˚C (Figure 13). This was due to the fact that the solution became more viscous at lower temperature. Hence, reducing the membrane surface coverage that resulted in lower flux increment due to higher energy dissipation.

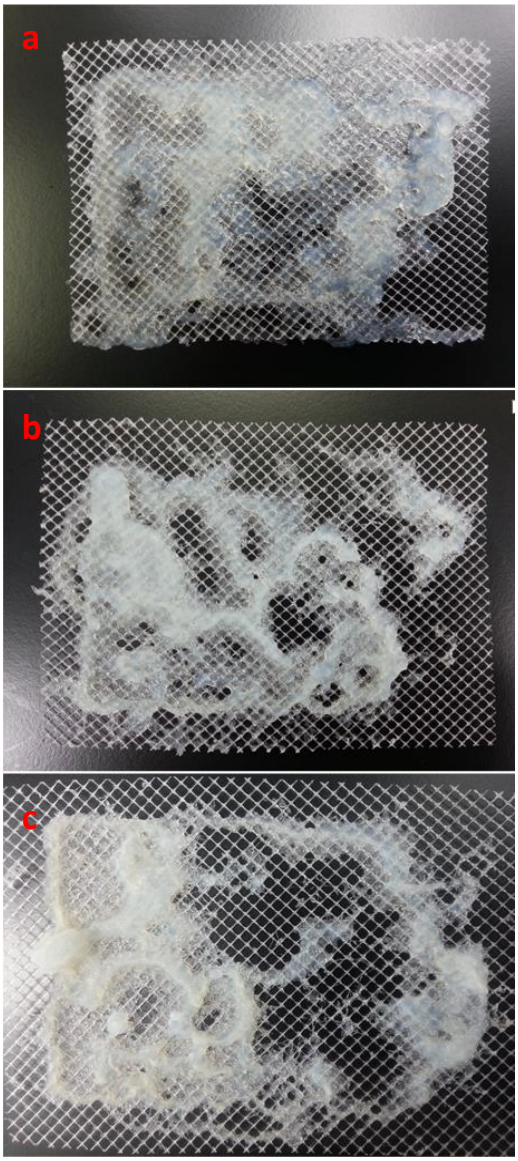

Figure 12. Images of spacer upon experiment at various saturation levels: (a) LS 15%+100 ppm ALG; (b) LS 50%+100 ppm ALG; (c) LS 100%+100 ppm ALG.

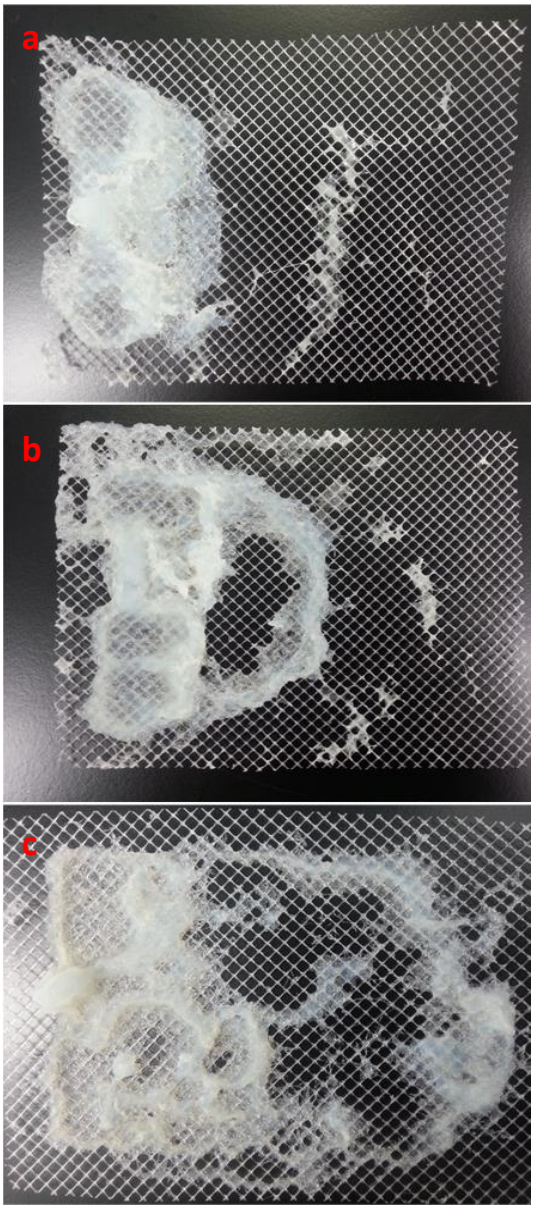

Figure 13. Images of spacer upon experiment with LS 100%+ALG at different feed temperatures: (a) 40˚C; (b) 55˚C; (c) 70˚C.

The morphology of membrane surfaces fouled by various substances can be seen in Figure 14. The membrane of LS 100%+ALG was covered with gel-like layer together with calcium sulfate crystals (Figure 14a). The membrane of LS 100%+BSA appeared to be relatively clean

(Figure 14b), while the membrane surface of LS 100%+XG was fully covered by flocs (Figure 14c). These images showed an agreement with the flux profiles in Figure 6.

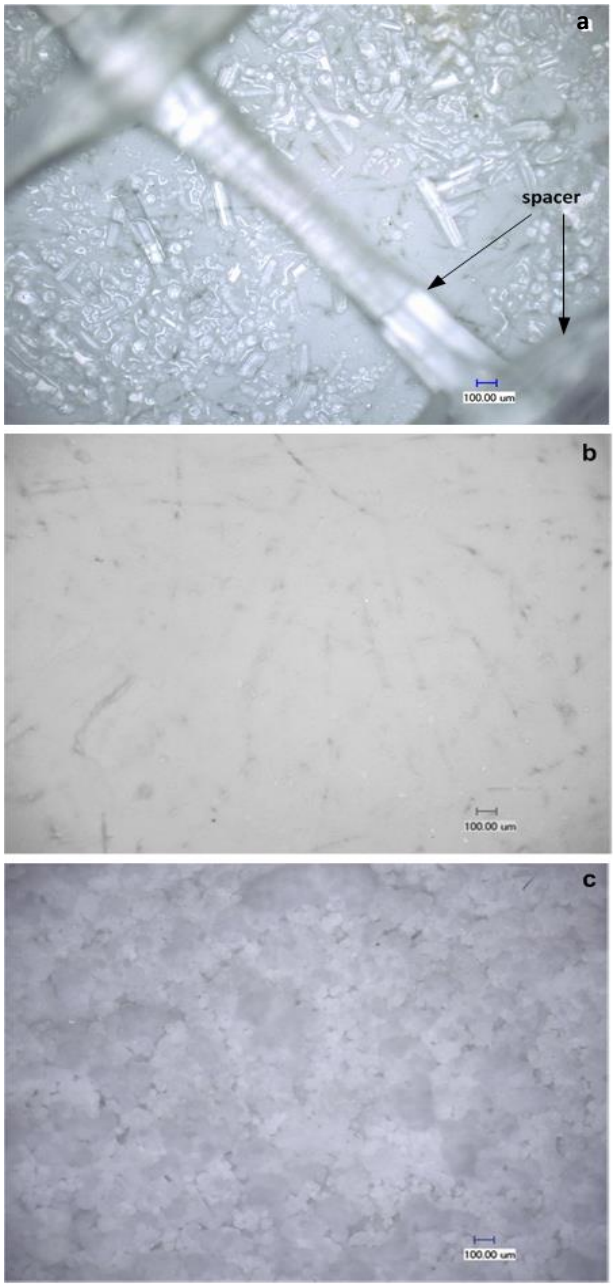

Figure 14. Images of membrane surface after experiments with (a) LS 100%+ALG; (b) LS 100%+BSA; (c) LS 100%+XG.

3.9. Mechanism of flux enhancing effect generated by alginate

MD is a thermally-driven process, and the mass transfer in MD is accompanied by heat transfer, which leads to evaporative cooling (dissipation of applied temperature difference) in the thermal boundary layer. Hence, the most suitable membranes for MD process should have low thermal conductivity to minimize heat loss due to sensible heat transfer. In the current study, the addition of alginate in the feed led to the formation of a calcium alginate gel (hydrophilic) layer on the membrane surface as shown in Figures 12-13. The thermal conductivity of alginate compound is 0.0242 W m^{-1} K^{-1} while [20], while the thermal conductivity of membrane material PTFE is 0.28 W m^{-1} K^{-1} [21]. Thus the presence of alginate reduced the thermal conductivity of alginate-membrane layer, which may hinder the dissipation of heat/thermal energy due to evaporative cooling or reduce conductive heat loss in the membrane, resulting in the improvement of process efficiency. This effect is similar to those obtained with Janus membrane [22].

Possible mechanism of flux enhancing effect by alginate is depicted in Figure 15. The efficiency of transport across the membrane in DCMD is governed by the boundary layer heat transfer. Temperature polarization coefficient (TPC) is commonly used to indicate the extent of the boundary layer resistance over the total heat transfer resistance [23]. TPC value approaches unity for a well-designed MD module. Low TPC values indicate high thermal boundary layer resistances. Our findings suggest that the formation of loose calcium alginate layer on the membrane surface may keep the temperature at the membrane surface (Tf, m) in a relatively higher level, enhancing the TPC due to less heat loss in the thermal boundary layer. This unique phenomenon has not been reported elsewhere.

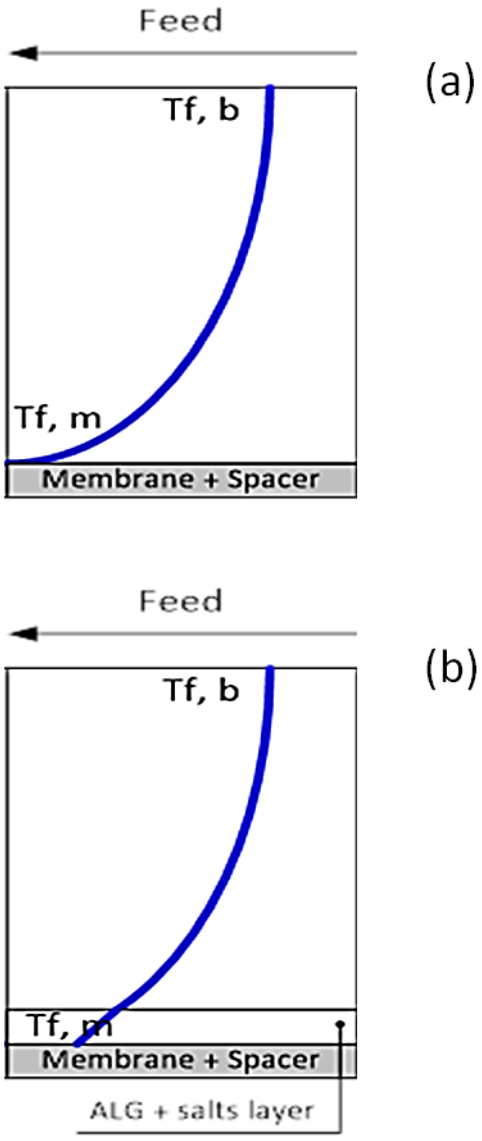

Figure 15. Mechanism of flux enhancing effect generated by alginate: a) the absence of calcium alginate layer; b) the formation of calcium alginate layer on the solid-liquid interface. (Tf, b –temperature of the feed bulk solution; Tf, m – temperature at the membrane surface; the blue line is the temperature profile in the thermal boundary layer).

4. Conclusions

Findings from this study showed that the efficiency of MD process could be altered by varying the feed properties/compositions and operating conditions. Certain combinations of common

fouling precursors, such as alginate and calcium under certain operating conditions could otherwise result in an unexpected flux improvement. The degree of improvement was governed by the consistency of the alginate gel layer formed, which in turn was determined by the compositions and types of substances present in the feed solutions, as well as the temperature. It is believed that the presence of a hydrophilic layer (calcium alginate gel) on top of the membrane could reduce the amount of heat dissipated due to evaporative cooling, thus enhancing the thermal efficiency of the system. Further studies are required to obtain better understanding of these interesting phenomena. The addition of alginate at a later stage could prevent further decline in MD performance, although the degree of improvement was not as much as when alginate was added since the beginning of the process. Based on the range of parameters studied, higher calcium content in feed, higher feed temperature (70^{o}C), and higher alginate concentration (100 ppm) promoted the formation of greater amount and less viscous gel aggregate, allowing the gel to smoothly cover the membrane surface, thus resulted in higher flux increment. This study also shows that it is not necessary for the hydrophilic layer to be embedded on the membrane, a loose hydrophilic layer could provide a similar flux enhancement effect.

Acknowledgements

The authors would like to acknowledge GE Energy for providing the PTFE membranes. Funding support from Singapore Economic Development Board to Singapore Membrane Technology Centre is gratefully acknowledged.

References

1. Findley, M.E., *Vaporization through Porous Membranes.* Industrial & Engineering Chemistry Process Design and Development, 1967. **6**(2): p. 226-230.
2. Findley, M.E., et al., *Mass and heat transfer relations in evaporation through porous membranes.* AIChE Journal, 1969. **15**(4): p. 483-489.
3. Blanco Gálvez, J., L. García-Rodríguez, and I. Martín-Mateos, *Seawater desalination by an innovative solar-powered membrane distillation system: the MEDESOL project.* Desalination, 2009. **246**(1-3): p. 567-576.
4. Susanto, H., *Towards practical implementations of membrane distillation.* Chemical Engineering and Processing: Process Intensification, 2011. **50**(2): p. 139-150.
5. Rehman, Z.U., et al., *Advanced characterization of dissolved organic matter released by bloom-forming marine algae.* Desalination and Water Treatment, 2017. **69**: p. 1-11.
6. Naidu, G., et al., *Organic fouling behavior in direct contact membrane distillation.* Desalination, 2014. **347**: p. 230-239.
7. Liu, C., L. Chen, and L. Zhu, *Fouling mechanism of hydrophobic polytetrafluoroethylene (PTFE) membrane by differently charged organics during direct contact membrane distillation (DCMD) process: An especial interest in the feed properties.* Journal of Membrane Science, 2018. **548**: p. 125-135.
8. Higgin, R., K.J. Howe, and T.M. Mayer, *Synergistic behavior between silica and alginate: Novel approach for removing silica scale from RO membranes.* Desalination, 2010. **250**(1): p. 76-81.
9. Mo, Y., et al., *A new perspective on the effect of complexation between calcium and alginate on fouling during nanofiltration.* Separation and Purification Technology, 2011. **82**(1): p. 121-127.
10. Zhou, J., et al., *Layer by layer chitosan/alginate coatings on poly(lactide-co-glycolide) nanoparticles for antifouling protection and Folic acid binding to achieve selective cell targeting.* Journal of Colloid and Interface Science, 2010. **345**(2): p. 241-247.
11. Wu, J., A.E. Contreras, and Q. Li, *Studying the impact of RO membrane surface functional groups on alginate fouling in seawater desalination.* Journal of Membrane Science, 2014. **458**: p. 120-127.
12. Arkhangelsky, E., et al., *Combined organic-inorganic fouling of forward osmosis hollow fiber membranes.* Water Research, 2012. **46**(19): p. 6329-6338.
13. Meng, S., H. Winters, and Y. Liu, *Ultrafiltration behaviors of alginate blocks at various calcium concentrations.* Water Research, 2015. **83**: p. 248-257.
14. Tow, E.W., et al., *Comparison of fouling propensity between reverse osmosis, forward osmosis, and membrane distillation.* Journal of Membrane Science, 2018. **556**: p. 352-364.
15. Boubakri, A., A. Hafiane, and S.A.T. Bouguecha, *Direct contact membrane distillation: Capability to desalt raw water.* Arabian Journal of Chemistry, 2017. **10**: p. S3475-S3481.
16. Qtaishat, M., et al., *Heat and mass transfer analysis in direct contact membrane distillation.* Desalination, 2008. **219**(1-3): p. 272-292.
17. Saroff, H.A. and M.S. Lewis, *The binding of calcium ions to serum albumin.* The Journal of Physical Chemistry, 1963. **67**(6): p. 1211-1216.
18. Schofield, R.W., et al., *Factors Affecting Flux in Membrane Distillation* Desalination, 1990. **77**: p. 279-294.

19. Jamal, S., S. Chang, and H. Zhou, *Filtration Behaviour and Fouling Mechanisms of Polysaccharides.* Membranes, 2014. **4**: p. 319-332.
20. Rbihi, S., et al., *Characterization and thermal conductivity of cellulose based composite xerogels.* Heliyon, 2019. **e01704**: p. 1-8.
21. Price, D.M. and M. Jarratt, *Thermal conductivity of PTFE and PTFE composites.* Thermochimica Acta, 2002. **392-393**: p. 231-236.
22. Yang, H.-C., et al., *Janus hollow fiber membrane with a mussel-inspired coating on the lumen surface for direct contact membrane distillation.* Journal of Membrane Science, 2017. **523**: p. 1-7.
23. Khayet, M., *Membranes and theoretical modeling of membrane distillation: A review.* Advances in Colloid and Interface Science, 2011. **164**(1): p. 56-88.

Figure and Table Captions.

Figure 1.	Schematic diagram of bench scale membrane distillation system.
Figure 2.	Permeate flux profiles at different ionic strengths (a. high salinity feed (HS); b. low salinity feed (LS); feed side at 70^{o}C and cool side at 20^{o}C).
Figure 3.	The influence of feed solution saturation level on MD process performance (feed side at 70^{o}C and cool side at 20^{o}C).
Figure 4.	Effect of feed temperature on MD process performance.
Figure 5.	Impact of alginate concentration on MD process performance (feed side at 70^{o}C and cool side at 20^{o}C).
Figure 6.	Influence of foulant nature on MD process performance (feed side at 70^{o}C and cool side at 20^{o}C).
Figure 7.	Comparison of MD performances with and without spacer for LS100% + ALG 100 ppm (feed side at 70^{o}C and cool side at 20^{o}C).
Figure 8.	The effect of alginate injection time on MD process performance (feed side at 70^{o}C and cool side at 20^{o}C).
Figure 9.	Comparison of MD performances with MilliQ water (MQ) and 100 ppm alginate solution as feed (ALG) (feed side at 70^{o}C and cool side at 20^{o}C).
Figure 10.	Viscosity of feed solutions as a function of shear rate.
Figure 11.	Digital images of membrane surfaces (a) pristine membrane; (b) upon experiment with HS 15%; (c) upon experiment with LS 15%; (d) image of the membrane with spacer upon experiment with LS 15%+ALG.
Figure 12.	Images of spacer upon experiment at various saturation levels: (a) LS 15%+100 ppm ALG; (b) LS 50%+100 ppm ALG; (c) LS 100%+100 ppm ALG.
Figure 13.	Images of spacer upon experiment with LS 100%+ALG at different feed temperatures: (a) 40˚C; (b) 55˚C; (c) 70˚C.
Figure 14.	Images of membrane surface after experiments with (a) LS 100%+ALG; (b) LS 100%+BSA; (c) LS 100%+XG.
Figure 15.	Mechanism of flux enhancing effect generated by alginate: a) the absence of calcium alginate layer; b) the formation of calcium alginate layer on the solid-liquid interface. (Tf, b –temperature of the feed bulk solution; Tf, m – temperature at the membrane surface; the blue line is the temperature profile in the thermal boundary layer).

Table 1. Composition of feed solutions used in the study (HS: high salinity; LS: low salinity)